

AFRL-AFOSR-UK-TR-2011-0007



Transition Control with Dielectric Barrier Discharge Plasmas

Cameron Tropea

**Technische Universitaet Darmstadt
Department of Mechanical Engineering
Petersenstrasse 30
Darmstadt, Germany 64287**

EOARD GRANT 08-3032

October 2010

Final Report for 01 August 2008 to 01 August 2010

Distribution Statement A: Approved for public release distribution is unlimited.

**Air Force Research Laboratory
Air Force Office of Scientific Research
European Office of Aerospace Research and Development
Unit 4515 Box 14, APO AE 09421**

REPORT DOCUMENTATION PAGE

Form Approved OMB No. 0704-0188

Public reporting burden for this collection of information is estimated to average 1 hour per response, including the time for reviewing instructions, searching existing data sources, gathering and maintaining the data needed, and completing and reviewing the collection of information. Send comments regarding this burden estimate or any other aspect of this collection of information, including suggestions for reducing the burden, to Department of Defense, Washington Headquarters Services, Directorate for Information Operations and Reports (0704-0188), 1215 Jefferson Davis Highway, Suite 1204, Arlington, VA 22202-4302. Respondents should be aware that notwithstanding any other provision of law, no person shall be subject to any penalty for failing to comply with a collection of information if it does not display a currently valid OMB control number.
PLEASE DO NOT RETURN YOUR FORM TO THE ABOVE ADDRESS.

1. REPORT DATE (DD-MM-YYYY) 28-10-2010	2. REPORT TYPE Final Report	3. DATES COVERED (From - To) 01 August 2008 - 01 August 2010
--	---------------------------------------	--

4. TITLE AND SUBTITLE Transition Control with Dielectric Barrier Discharge Plasmas	5a. CONTRACT NUMBER FA8655-08-1-3032
	5b. GRANT NUMBER Grant 08-3032
	5c. PROGRAM ELEMENT NUMBER 61102F

6. AUTHOR(S) Professor Cameron Tropea A. Duchmann S. Grundmann	5d. PROJECT NUMBER
	5d. TASK NUMBER
	5e. WORK UNIT NUMBER

7. PERFORMING ORGANIZATION NAME(S) AND ADDRESS(ES) Technische Universitaet Darmstadt Petersenstrasse 30 Darmstadt, Germany 64287	8. PERFORMING ORGANIZATION REPORT NUMBER N/A
--	--

9. SPONSORING/MONITORING AGENCY NAME(S) AND ADDRESS(ES) EOARD Unit 4515 BOX 14 APO AE 09421	10. SPONSOR/MONITOR'S ACRONYM(S) AFRL/AFOSR/RSW (EOARD)
	11. SPONSOR/MONITOR'S REPORT NUMBER(S) AFRL-AFOSR-UK-TR-2011-0007

12. DISTRIBUTION/AVAILABILITY STATEMENT
Approved for public release; distribution is unlimited.

13. SUPPLEMENTARY NOTES

14. ABSTRACT

The long-term objective of the project is to control natural boundary-layer transition through the use of plasma actuators. Transition delay or even suppression has its merits not only in lower wall shear stress and frictional drag of laminar as opposed to turbulent boundary layers, but transition control can be instrumental in influencing flow separation, which opens avenues for significantly influencing pressure drag and wake acoustics of bluff bodies or profiles.

The focus of the project is on understanding fundamentals of the transition control and on optimization of actuator design and operating parameters. The project is of experimental nature and is composed of three periods. During the first period, improved plasma actuators are developed for boundary-layer control. A small wind tunnel, optimized for high resolution laser optical measurements in boundary layers, was constructed and will yield precise knowledge of the flow field and volume force distribution of different actuator geometries for developing advanced actuators for transition control. These actuators will be used in a larger tunnel under pressure-gradients encountered in flight situations during the second period to enhance the design and to achieve a reliable delay of transition. The development of a feedback control circuit for active wave cancelation using pulsed plasma actuators will also be conducted in the second period. Finally, all developed technologies will be applied in the third period for in-flight experiments, demonstrating the delay of transition on the wing of a full size motorized glider.

15. SUBJECT TERMS
EOARD, Flow Control, Plasma Aerodynamic, Boundary Layer transition

16. SECURITY CLASSIFICATION OF:			17. LIMITATION OF ABSTRACT SAR	18. NUMBER OF PAGES 37	19a. NAME OF RESPONSIBLE PERSON Gregg Abate
a. REPORT UNCLAS	b. ABSTRACT UNCLAS	c. THIS PAGE UNCLAS			19b. TELEPHONE NUMBER (Include area code) +44 (0)1895 616021

Transition Control with Dielectric Barrier Discharge Plasmas

Dipl.-Ing. A. Duchmann
Dr.-Ing. S. Grundmann
Prof. Dr.-Ing. C. Tropea



TECHNISCHE
UNIVERSITÄT
DARMSTADT



CSI

End of Phase Report
Period 1

Award No. FA8655-08-1-3032

Abstract

The long-term objective of the project is to control natural boundary-layer transition through the use of plasma actuators. Transition delay or even suppression has its merits not only in lower wall shear stress and frictional drag of laminar as opposed to turbulent boundary layers, but transition control can be instrumental in determining flow separation, which opens avenues for significantly influencing pressure drag and wake acoustics of bluff bodies or profiles.

The focus of the project is on understanding fundamentals of the transition control and on optimization of actuator design and operating parameters. The project is of experimental nature and is composed of three periods. During the first period, improved plasma actuators are developed for boundary-layer control. A small wind tunnel, optimized for high resolution laser optical measurements in boundary layers, was constructed and will yield precise knowledge of the flow field and volume force distribution of different actuator geometries for developing optimized actuators for transition control. These actuators will be used in a larger tunnel during the second period to optimize the design and to achieve a reliable delay of transition. The development of a feedback control circuit for active wave cancelation using pulsed plasma actuators, will also be conducted in the second period. Finally, all developed technologies will be applied in the third period for in-flight experiments, demonstrating the delay of transition on the wing of a full size motorized glider.

This report complements the interim report provided after the first half of the first period and provides an overview over the accomplishments realized during the first period of the project.



Contents

1	Introduction	3
2	Hot wire measurements of test section flow	3
3	Steady DBD actuation	5
4	Starting behavior in quiescent air	6
5	Active wave cancelation	8
6	Glider plane preparations	10
7	Linear stability analysis	12
8	Outlook	13
9	Publications	14

1 Introduction

During the first period of the project, the main objective is to enhance the understanding of the plasma physics governing the effects of DBD actuators. The spatial and temporal distribution of the induced body force is not known and the driving mechanisms not yet understood. Laser optical measurements in the vicinity of the actuators are conducted to highly resolve the spatial velocity distribution of the induced flow field. The PIV measurements are accompanied by an investigation on the influence of geometry and materials of the DBD actuator on the created flow patterns. For these purposes, the actuator is operated in quiescent air. The aim of the project is to successfully apply DBD actuation for boundary-layer control. Therefore, the effect of the actuator has to be determined and investigated inside boundary-layer flows of different types. In order to assess the mechanisms of momentum addition to the lower regions of the boundary layer, PIV measurements are conducted on a flat plate installed in a newly constructed wind tunnel. The wind tunnel was designed to provide optimal accessibility by optical measurement techniques and to allow easy and variable changes of the setup (pressure gradient, length of the flat plate inside the test section, upstream flow conditioning elements).

Besides these investigations to determine the effect of constantly operated DBD actuators, an enhancement of the active wave cancelation (AWC) of Tollmien-Schlichting waves (TS-waves) is aimed for. Earlier experiments at TU Darmstadt [2] confirmed the concept of using DBD actuation to dampen artificially generated wavelike structures in laminar boundary-layer flows of velocities up to 10m/s.

Such investigations are foreseen to be taken to the in-flight experimental level. The aim is to obtain more realistic boundary conditions such as turbulence levels and Reynolds numbers for possible applications beyond windtunnel tests.

2 Hot wire measurements of test section flow

The construction of a newly built, specially designed low-turbulence windtunnel dedicated to the investigations of this project has been described in the first interim report after the first half of the first period (May 2009). The test section spans 600mm in streamwise direction (x). With respect to the setup of the flat-plate experiments described in Chapter 3, the 240mm wide lateral dimension is denominated wall-normal (y) whereas the spanwise dimension (z) measures 180mm. After completion of the windtunnel, measurements on the flow quality inside the test section have been conducted. The results of these investigations are presented in the following.

For the basic experiments of the project's first phase, boundary-layer flow on a flat plate at freestream velocities up to 15m/s is needed. The test section flow has to be known in terms of turbulence intensity as well as blockage effects next to the tunnel walls. A single-wire constant temperature anemometry setup was chosen to take single-point, time-resolved velocity measurements. In order to access the complete volume of the test section, a 2-axis *Velmex BiSlide* traversing system was acquired and installed. The traversing mechanism allows positioning the probe within the x, y -plane. The spanwise position is zero in the center of the test section, considering the assumed two-dimensionality of the flat-plate investigations and referring to the plane illuminated by the laser sheet during the Particle Image Velocimetry (PIV) investigations.

In order to access z -positions different to zero, the probe has to be adjusted manually. This is facilitated by an easily-accessible construction of the probe support structure.

Different flow velocities between 3 and 15m/s have been applied by running the radial compressor downstream of the test section at variable revolution speeds. The flow inside the test section has been evaluated to be homogeneous and symmetric. Although the inlet of the wind-tunnel is situated inside a room and not evenly spaced from the room walls in all directions, the test section flow does not show any related effects. The ratio of $n = \frac{100}{9}$ of the Börger-type contraction is well-suited to reduce the turbulence intensity to an acceptable level for an open-circuit windtunnel without special precautions (e.g. acoustic insulation).

The effect of the windtunnel walls, increasing with streamwise propagation, can be identified in Figure 2.1. The turbulence intensity $Tu = \frac{u_{RMS}}{U}$ is plotted at four x, y -planes ($z = 0\text{mm}, 30\text{mm}, 60\text{mm}, 86\text{mm}$) for two exemplary freestream velocities. Thereby it gives an impression of the turbulence distribution across half of the overall test section (x, y -planes at negative z -values proved to be symmetric to the positive ones and are not plotted). Zones of high turbulence intensity indicate the shear layer formation provoked by the walls. In the upper part of the plots, the position next to the lateral windtunnel wall is presented. It shows a significant wall interference effect for flow speeds above 12m/s. The tunnel centerline flow can be found in the lowest intersection. It becomes obvious that for the shown flow velocities the test section flow becomes constricted downstream of $x = 400\text{mm}$ such that the assumption of 2D flow may be violated. For this reason, measurements will be limited to the test-section area from $x = 0 - 400\text{mm}$.

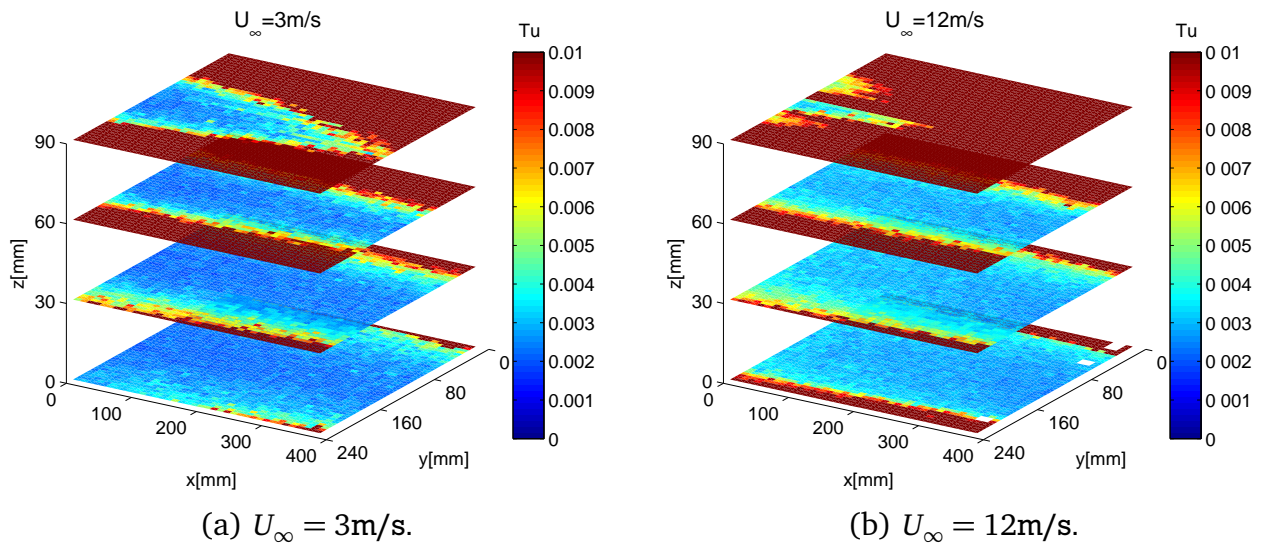


Figure 2.1: Test section flow turbulence intensity at a) $U_\infty = 3\text{m/s}$ and b) $U_\infty = 12\text{m/s}$.

The maximum turbulence intensity inside the test-section regions not affected by the walls is $Tu = 0.3\%$. Such low freestream turbulence enables measurement of laminar boundary-layer flow where the transition process is not governed by bypass transition but natural Tollmien-Schlichting waves.

3 Steady DBD actuation

The experimental setup and the construction of a windtunnel specially designed for these experiments have been discussed in the last interim report. The investigations during the second half of the first period concentrated on obtaining fundamental data on the influence of steadily operated DBD actuators on quiescent air and laminar boundary-layer flows of different types. The first task was to refine the PIV setup to guarantee reliable data acquisition of all flat-plate investigations. One challenge is to provide adequate seeding in the viscous sublayer of a laminar boundary-layer. This is fundamental to quantify the actuator effect based on characteristic boundary-layer properties like displacement thickness δ_1 , momentum thickness δ_2 and shape factor H_{12} . The evolution of the boundary-layer profiles downstream of the actuator position is a function of the actuator geometry as well as the operation voltage. The penetration depth denominates the zone of influence of the actuator in wall-normal direction. The streamwise directed zone where the body force affects the flow is limited by the lower (buried) electrode in conventional setups. Nevertheless, the effect on the flow field can be noticed further downstream.

The preliminary investigations described in the former interim report have been extended to parametrical studies of DBD actuators influencing laminar boundary-layer flows of various velocities. A conventional setup of the actuator with an upper electrode width of 2mm and a lower electrode width of 10mm was chosen. The dielectric barrier is formed by 5 layers of adhesive Kapton tape and has a total thickness of $300\mu\text{m}$. The spanwise oriented actuator is placed 260mm downstream of the elliptical leading edge of the flat plate and powered by a *Minipuls 1*.

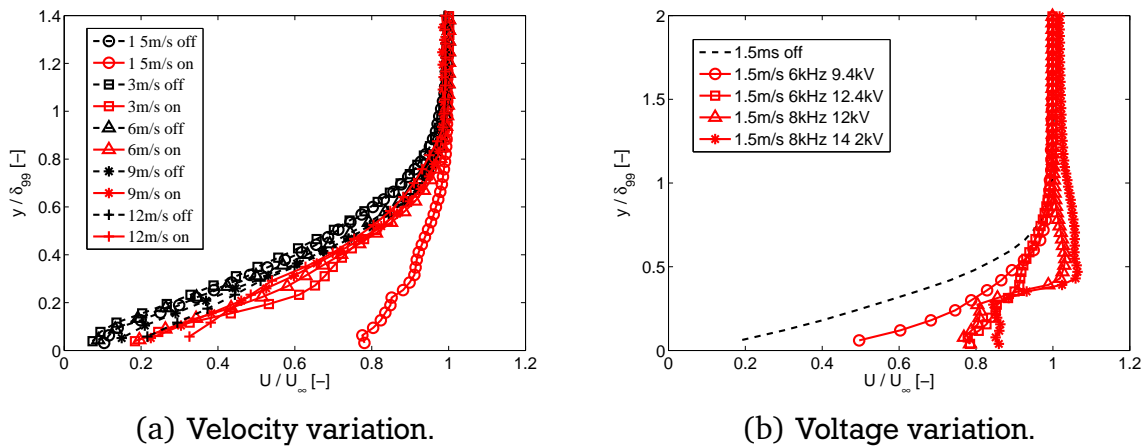


Figure 3.1: Boundary-layer profiles (with and without DBD actuation) 5mm downstream of actuator position under variation of a) freestream velocity and b) actuator voltage.

The mean flow velocity inside the test section for the presented experiments was changed between 3 and 15m/s. For lower velocities it is easier to identify the shape change of the boundary-layer profiles from the PIV data. An overview of the obtained profiles with and without actuation is shown in Figure 3.1 (a). It can be clearly seen that the visible distortion of the velocity profile is highly dependent on the free-stream velocity. For higher velocities only the derivatives of the profiles show larger variations. Since the derivatives with respect to the

wall-normal coordinate are inputs for linear stability analysis (refer to Chapter 7), these can be used to determine the effect on the flow field.

Another strong dependency is depicted in Figure 3.1 (b). This plot indicates the increase of added momentum with higher operation frequencies. For the 8kHz cases, the deviation of the mean velocity profile from the DBD-unaaffected case is more evident between the outer limit of the boundary layer and half its thickness ($\frac{y}{\delta_{99}} \approx 0.5$). An overshoot of the velocity profile can be seen for the higher frequency cases, indicating that the momentum addition is badly matched for such low velocity boundary-layer flow. A profile as shown here would be more receptive to transition promoting disturbances.

4 Starting behavior in quiescent air

In order to understand the unsteady behavior of the DBD actuator and especially the effects related to the pulsed-mode operation, it is necessary to acquire data on the velocities induced in quiescent air next to the actuator. For a short period of time a special PIV system became available to investigate the periodic actuator operation on high temporal resolution. To understand the modulated forcing of pulsed operation needed for the active wave cancellation (see Chapter 5), PIV images were taken at a frequency of 1 and 10kHz.

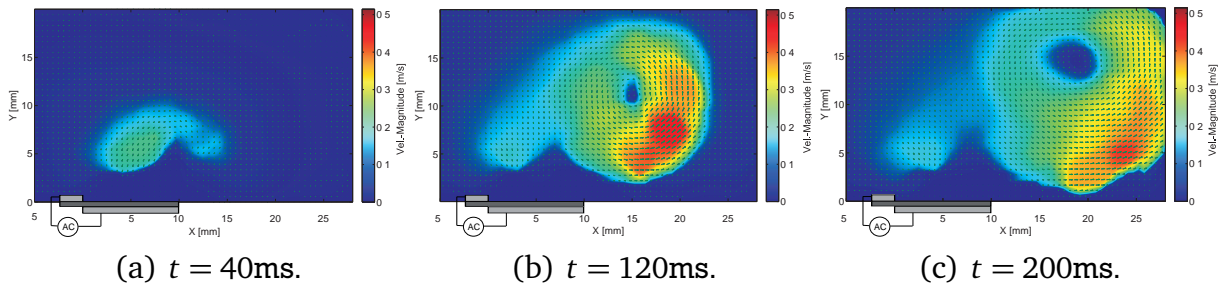


Figure 4.1: Behavior of starting vortex after onset of actuator operation [$t = 0$ ms] for $V_{pp} = 8$ kV, $DC = 10\%$, $w = 2.5$ mm.

When initiating DBD actuation in quiescent air, a starting vortex is created. Figure 4.1 illustrates the velocity field induced due to the actuator operation. Directly after turning on the high-voltage power-supply (a), the starting vortex is created (b) and convected away from the actuator position (c) until it slowly decays and leaves the field of view.

The features of the starting vortex provide useful information about the strength of the momentum coupling and the instationary actuator behavior. Care has to be taken when identifying vortical structures in unsteady velocity fields. A filtering method was applied to distinguish between the starting vortex and the wall-near shear layer in order to follow the vortex trajectory. A systematic investigation of varying actuator voltages, duty cycles and operation frequencies was undertaken to explore the effect on the spatial and temporal vortex development.

Figure 4.2 (a) shows example results of the temporal evolution of the out-of-plane vorticity magnitude $|\vec{\omega}|$ under variation of duty cycle and width of the exposed electrode. The actuator operates at a fixed frequency and input voltage of $f = 9.5$ kHz and $V_{pp} = 9$ kV, the modulation

frequency for pulsed operation is $f_{mod} = 100\text{Hz}$. The characteristic temporal development of the vorticity can be empirically described by

$$|\vec{\omega}|_{core}^{(t)} = \alpha_t + \beta_t t e^{-\frac{t}{\tau_t}}. \quad (4.1)$$

Directly after the onset of actuator operation, the vorticity magnitude $|\vec{\omega}|$ rises linearly. After several plasma cycles of steady or pulsed operation a maximum is reached, followed by a subsequent exponential decay while the vortex is convected away from the actuator. As the duty cycle in pulsed operation is increased, the momentum transfer into the fluid is raised, leading to higher vorticity values in the vortex core. Figure 4.2 (a) also indicates that for the 7.5mm wide exposed electrode, the vorticity values are lower than for a smaller electrode of $w = 2.5\text{mm}$. The temporal evolution of the vortex core position shows that for 7.5mm wide exposed electrodes no clearly defined starting vortex is created and that vorticity maxima are found along the shear-layer of the forming wall-jet.

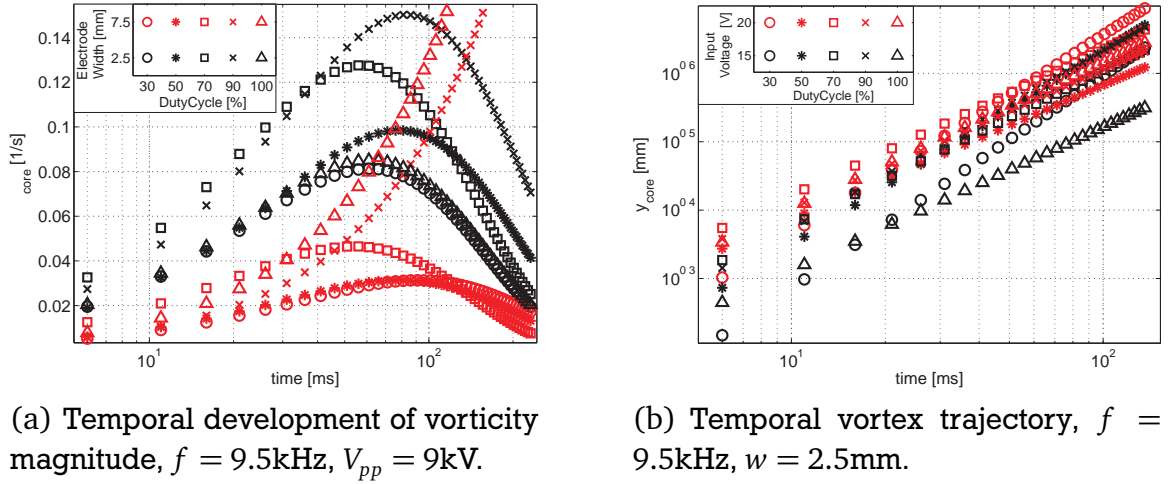


Figure 4.2: Temporal vortex development.

Figure 4.2 (b) illustrates the dependence of the temporal vortex trajectory on the operating voltage and frequency. The wall-normal coordinate of the vortex core is plotted over time. The trajectories for the different setups all show a behavior described by

$$y_{core}(t) = b_t t^{a_t} \quad (4.2)$$

which was proposed by Allen and Naitoh [1] for characterization of size and velocity distribution of impulsively started vortex structures. The exponent a_t represents the slope of the curves in Figure 4.2 (b). The parameter dependent values a_t and b_t computed from the data are presented in Tables 4.1 and 4.2.

V_{pp}/DC	30%	50%	70%	90%	100%
9 kV	0.3104	0.2834	0.2268	0.2601	0.2100
12 kV	0.2904	0.1956	0.2140	0.2020	0.2154

Table 4.1: a_t [1/ms].

V_{pp}/DC	30%	50%	70%	90%	100%
9 kV	0.9452	1.1642	1.4141	1.2971	1.2636
12 kV	1.1898	1.5545	1.6127	1.5877	1.5332

Table 4.2: b_t [$1/\text{ms}^2$].

For a duty cycle of 30% (indicated by circles), a_t is higher than for steady operation (100% DC, triangles). The coefficient b_t exhibits a different trend. These tendencies suggest that for high duty cycles the vortex is created immediately after initiation (high b_t) and is quickly being convected in x-direction. At low DC, the build-up of the vortex takes more time because of limited momentum addition. This creates a large coherent structure which is lifted away from the wall faster (high a_t) than a small and strong vortical structure as created at high DC.

Whalley [6] examined the temporal development of the vortex core position for three actuator configurations, each yielding different power curves with regard to t^{a_t} . The current investigation is one step towards universal scaling of DBD actuators and the induced flow conditions.

5 Active wave cancelation

DBD actuators have been successfully applied for transition delay in boundary-layer flows of up to $U_\infty = 10\text{m/s}$ [2]. The Reynolds numbers at these speeds are yet well below values for in-flight conditions. Nevertheless, the concept of using DBD actuators for damping disturbances which cause the breakdown to turbulence has been proven by windtunnel experiments and confirmed numerically by Quadros [4].

Recent investigations conducted in the framework of a Master's thesis have concentrated on increasing the freestream speeds where Tollmien-Schlichting waves inside a laminar boundary layer can be attenuated. The tests are conducted in the bigger open-circuit windtunnel existent at TU Darmstadt which is further described in [2]. The newly-built windtunnel described in Chapter 2 is not suitable for these measurements due to the limited test section length. Natural transition does not even occur within the 1.6m of the test section length of this windtunnel, therefore controlled boundary-layer stability experiments are conducted. The flat-plate setup for the investigations is depicted in Figure 5.1.

Disturbances are introduced on the flat plate 400mm downstream of the elliptical leading edge by a vibrating strip coupled to a coil actuator. In order to excite natural TS-wave frequencies dominating transition at flow speeds between 10 and 25m/s, the metallic strip is moved up and down at 100 to 200Hz. Low amplitudes are sufficient to excite the receptive boundary-layer. Downstream of the excitator, a hot-wire probe (sensor 1) is installed and determines the frequency of the incoming disturbance wave.

A DBD actuator is placed 150mm downstream of the disturbance source to counteract the incoming wavelike disturbances as illustrated in Figure 5.2. The flow structure induced by the DBD actuator (as described in the former interim report) is used to reduce the upstream directed flow pattern of the TS-wave.

Further downstream, a second hot-wire sensor (sensor 2) analyzes the amplitude of the velocity fluctuation, measuring the effectiveness of the wave cancelation by comparing it to the scenario without DBD actuation. The measured wave amplitude serves as an input for a control algorithm implemented in the *LabVIEW Real-Time* software environment. The controller com-

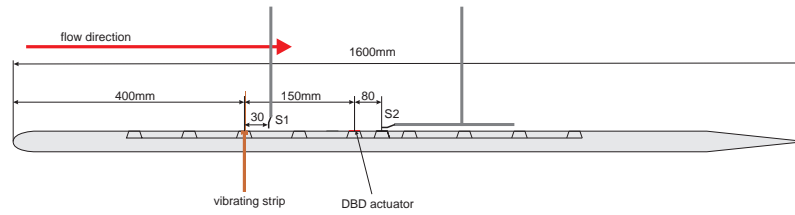


Figure 5.1: Flat-plate setup for active wave cancellation experiments.

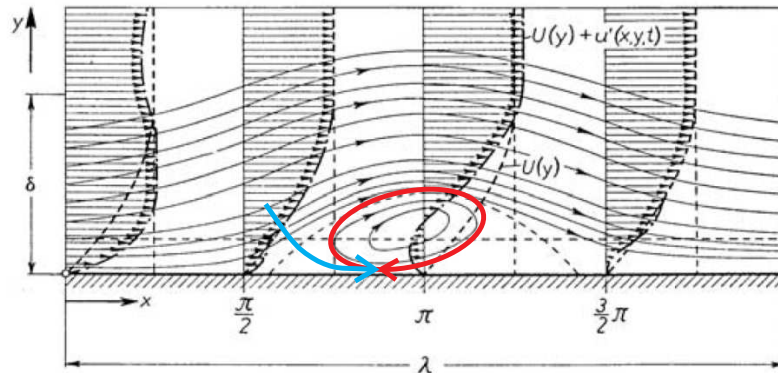


Figure 5.2: Damping of Tollmien-Schlichting waves in boundary-layer flow by DBD actuator. Red: TS-Wave, Blue: DBD actuation.

parses the signal of the wave disturbance and calculates an output signal for the DBD power supply. The modulation frequency of this signal has to be equal to the frequency measured at sensor 1, but its amplitude, the duty cycle and phase relation remain unknown. Several optimization schemes were developed by Quadros [4], optimizing the variable parameters to obtain a maximized reduction of the disturbance. The control algorithms were implemented into the experimental setup and successfully applied for TS-wave cancellation. A sketch indicating the controller setup is shown in Figure 5.3.

The root-mean-square voltage signal of sensor 2 for a freestream windtunnel velocity of $U_\infty = 25\text{m/s}$ is plotted over time in Figure 5.4. The grey zones indicate that the control algorithm is running, powering the DBD actuator to dampen the incoming disturbance. Almost immediately after initiation of the control mechanism, the amplitude of the disturbance wave is reduced, pointing out the good performance of the algorithm to quickly adopt amplitude and phase relation and optimize the wave cancellation. Two different optimization schemes were tested within the experimental setup and showed comparably good results. The advantage of the most recently developed algorithm, which is based on the Nelder-Mead method, is its capability to use an arbitrary number of input variables for the optimization process.

By using these newly developed control methods, it has become feasible to apply the active wave cancellation for windtunnel freestream velocities up to 25m/s. A further increase in speed should be possible as the necessary amount of DBD induced momentum does not scale with the freestream velocity but rather with the disturbance amplitude - which is very small in the early linear stage. The limiting factor for a further increase of velocity for successful wave cancellation is the geometric setup of the flat-plate in the windtunnel. For higher speeds, the excitation as well as the damping of the waves have to take place further upstream because the transition

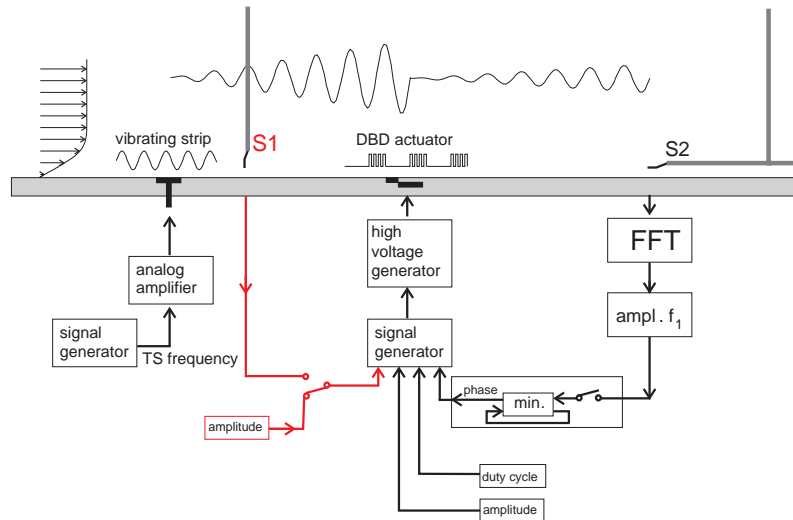


Figure 5.3: Working principle and input parameters for the controller unit.

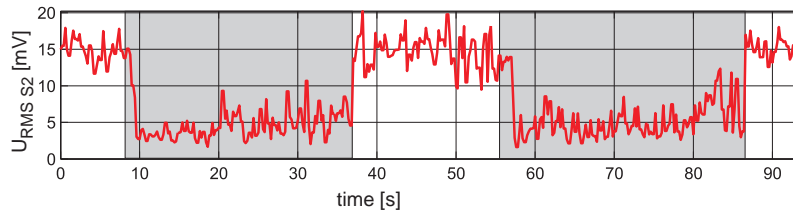


Figure 5.4: Amplitude of TS-wave over time for $U_{\infty} = 25\text{m/s}$, shaded in grey: DBD actuator on.

process is completed earlier. In order to succeed in the cancellation of waves at speeds above 30m/s , a new flat-plate setup has to be used. This new plate has been planned and is in the process of being manufactured. The work on the wave cancellation will be continued as soon as the new setup becomes operational.

The increase in velocity from 10m/s to 25m/s has been easily accomplished by implementing a new control strategy. Therefore it should be straightforward to further raise the freestream speeds by the factor of 2, reaching for the speeds encountered in in-flight experiments. The attempt to dampen TS-waves under flight conditions on a laminar wing by using DBD actuators are planned within the framework of this project.

6 Glider plane preparations

The project plan stipulates in-flight experiments on DBD based flow control during the third period. Since such experiments need long-term preparations and acquisition of specialized hardware, work on the experimental apparatus has already been initiated during period 1. In order to convey the boundary-layer control windtunnel experiments to the in-flight environment on the Grob G109 motorized glider available at TU Darmstadt, a special wing glove has to be built. This device covers part of the original glider wing and provides space and surface for implementation of experimental equipment. Figure 6.1 illustrates how the glove (1) will be placed on the plane's wing.

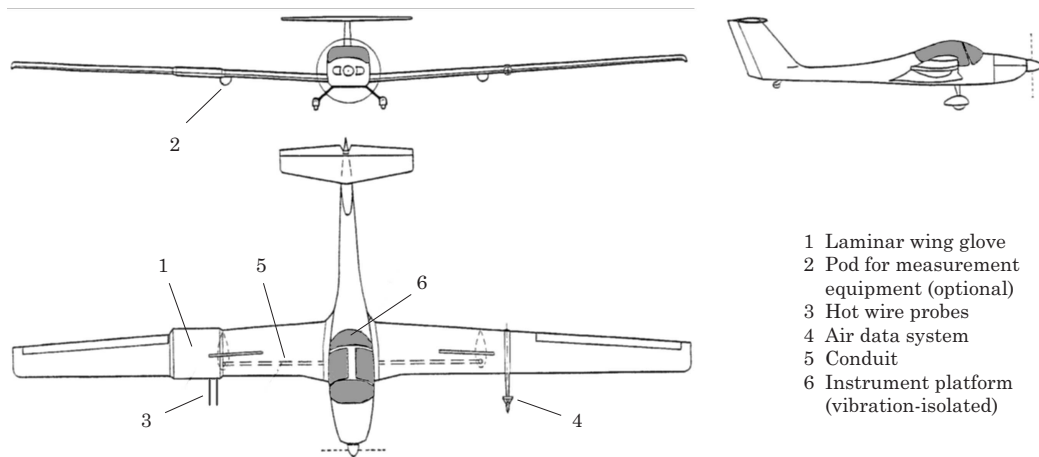


Figure 6.1: G109 motorized glider with wing glove.

The wing glove is designed to have a fully laminar profile like the wing profile and to provide the same lift as the wing area covered by the glove. Therefore a modified version of the Althaus AH 93157 profile for laminar glider wings is chosen. The total glove area is $1.35\text{m} \times 1.35\text{m}$ in spanwise and streamwise direction. Sloped side parts enable a smooth transition to the wing surface without notable pressure gradients. A plot of the pressure distribution across the wing area as taken from *FLUENT* calculations during the design process is shown in Figure 6.2. The wing glove is being used in various projects at TU Darmstadt such that an exchangeable insert (spanwise width 400mm) forms the center part of the glove, permitting access to the profile's suction as well as the pressure side for experiments.

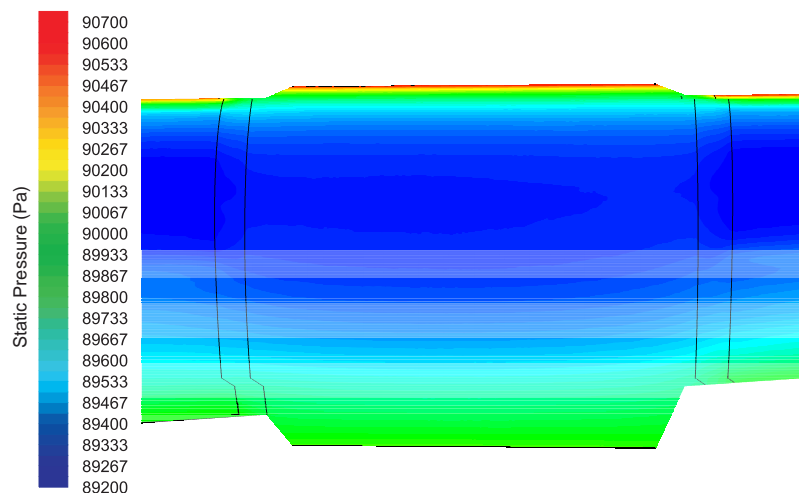


Figure 6.2: Computed pressure distribution on glove suction side ($U_\infty = 36\text{m/s}$).

Along the chord of the glove, pressure tabs are applied to allow for a measurement of the pressure distribution. A traversing system will render possible the acquisition of boundary-layer data on changing positions. An additional wake rake will facilitate the calculation of drag changes due to the flow control devices projected on the surface.

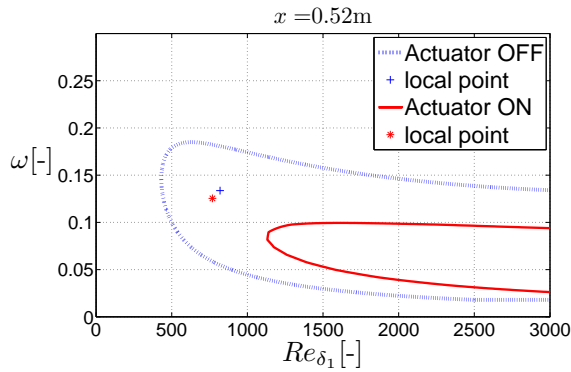
At this point, hot wire data acquisition appears most suitable to characterize the effect of DBD actuators placed on the glove insert. A new micro-welding instrument was acquired to allow for special configurations of hot-wire arrays on the glove surface. The exchangeable insert will be equipped with an array of hot wires downstream of the DBD actuators. Its surface will consist of a metallic material and grooves will be edged into it such that hot wires can be welded between the two edges of a groove. The setup will enable the application of DBD actuators for active wave cancelation as well as boundary-layer profile modification experiments at flight speeds between 25 and 50m/s.

At present the manufacturing of the glove molds is taking place. A CNC-milling machine has been acquired and the CAD data of the glove design exported to automate the manufacturing process of the high-precision molds. After completion of the molds for the upper and lower wing surface, the glove itself will be made from epoxy-resin reinforced glass fiber. An additional project is actually running at TU Darmstadt to investigate receptivity of the wing boundary-layer in regards to freestream turbulence, employing the new glove. These experiments will be very helpful to interpret the results from DBD actuation on the wing glove. Although these investigations are scheduled for period 3 of the project, preparations for the DBD inserts for the wing glove are already under way. The insert will account for the DBD power supply being installed next to the electrodes as well as implementation of hot wire anemometry equipment in the vicinity of the actuator.

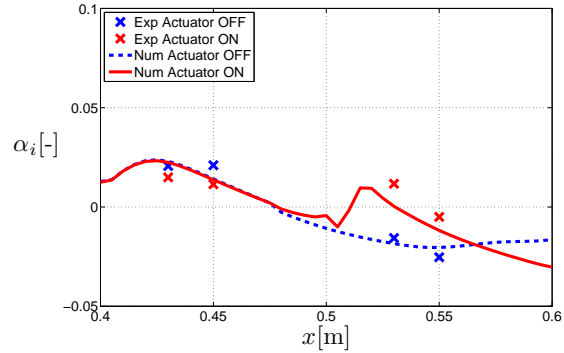
7 Linear stability analysis

As part of an undergraduate thesis project, a code for linear stability analysis (LSA) for laminar boundary-layers was developed. Numerical data as well as experimentally acquired boundary-layer profiles have been used as input for this code to calculate the stability properties of the flow [5]. Figure 7.1 (a) illustrates the calculated neutral stability curve for one boundary-layer profile downstream of the actuator position. The neutral stability curve separates the combinations of Reynolds number and wave frequency for which the wave disturbances are not amplified from the ones which lead to transition. The instability area of the boundary layer influenced by DBD actuation is significantly smaller than the area for the unaffected flow. This indicates that the actuator has a stabilizing influence on the boundary-layer profile. By applying the stability method to data on active wave cancelation it was discovered that even for pulsed operation of the DBD actuator, a stabilizing effect on the boundary-layer can be noted. Considering the streamwise propagation of disturbance amplitudes, Figure 7.1 (b) shows the amplification rate of the TS wave to be diminished (indicated by the raise of the curve towards positive values) by DBD actuation.

These findings reaffirm the positive influence of DBD actuation on laminar boundary-layers to delay the transition process. The method developed will be used to characterize different actuator setups and the induced effects on boundary layers under varying pressure gradients. The stability analysis will help in understanding the momentum coupling of newly developed actuator configurations like Sliding Discharge and streamwise arrays.



(a) $U_\infty = 3\text{m/s}$.



(b) $U_\infty = 12\text{m/s}$.

Figure 7.1: Linear stability analysis outputs: a) Neutral stability curve for laminar boundary-layer profile 20mm downstream of DBD actuator ($U_\infty = 8\text{m/s}$), b) Development of wave amplification rate over streamwise direction.

8 Outlook

A very successful international workshop on "Modeling Strategies for DBD Actuators" took place at TU Darmstadt in December 2008, sponsored by EOARD. The discussions and presentations by leading DBD scientists provided motivation and ideas for further investigations at the interface of plasma physics and flow control.

One approach to extend the influence of the actuator is to add an additional electrode to the setup which is biased by a DC voltage. The constant electric field is expected to promote the acceleration of ionized molecules and enhance the net-force introduced by the actuation. This technique is called Sliding Discharge and preliminary tests as well as experiments by other research groups [3] have shown remarkable improvement of the actuator effectiveness. Further ideas focus on using consecutive actuators forming an streamwise array of DBD devices. With such setups it will be possible to accelerate and stabilize the boundary layer much smoother without such singular acceleration events as they occur when single, strong actuators are used, at the same time reducing the necessary input power. Investigations on these configurations are conducted right now and will be available for presentation in the next interim report.

The second period of the project will enable a refined look at the influence of the DBD actuator on laminar and transitional flow in the windtunnel experiments. The investigation of new actuator setups will yield input on how to optimize the flow control devices for diverse applications. Improved actuators for application at higher velocities are being tested and put on the newly developed wing glove of the G109 glider plane. These investigations aim on applying DBD actuators under real flight conditions and atmospheric turbulence intensities, taking the plasma research from windtunnel tests to a next level.

9 Publications

Duchmann, A., Kriegseis, J., Grundmann, S., Tropea, C.: Customizing DBD Actuators for Flow-Control Applications using PIV. *8th International Symposium on Particle Image Velocimetry*, Melbourne, Australia, August 25-28, 2009. (accepted)

Duchmann, A., Reeh, A., Quadros, R., Kriegseis, J., Tropea, C.: Linear Stability Analysis for Manipulated Boundary-Layer Flows using Plasma Actuators. *IUTAM Symposium on laminar-turbulent transition*, Stockholm, Sweden, June 23-26, 2009.

Güttler, A.: Entwicklung effizienter Regel-Konzepte zur aktiven Dämpfung von Tollmien-Schlichting-Wellen mit Hilfe von Plasma-Aktuatoren. *Master's Thesis*, TU Darmstadt, 2009.

Bibliography

- [1] Allen, J. J., Naitoh, T. (2007): Scaling and instability of a junction vortex. *Journal of Fluid Mechanics*, **574**, 1–23.
- [2] Grundmann, S. (2008): Transition Control using Dielectric-Barrier Discharge Actuators. *Ph.D. Thesis* Institute of Fluid Mechanics and Aerodynamics, TU Darmstadt.
- [3] Louste, C., Artana, G., Moreau, E., Touchard, G. (2005): Sliding discharge in air at atmospheric pressure: electrical properties. *Journal of Electrostatics*, **63**, 615-620.
- [4] Quadros, R., Grundmann, S., Tropea, C. (2008): Numerical investigations of the boundary-layer stabilization using a phenomenological plasma actuator. *Journal of Flow, Turbulence and Combustion* (accepted).
- [5] Duchmann, A., Reeh, A., Kriegseis, J., Tropea, C. (2009): Linear Stability Analysis for Manipulated Boundary-Layer Flows using Plasma. *Seventh IUTAM Symposium on Laminar-Turbulent Transition*, Stockholm, Sweden, June 23-26.
- [6] Whalley, R., Jukes, T., & Choi, K.-S. (2008): On the development of a starting vortex in still air at the initiation of DBD plasma. *Proc. European Drag Reduction and Flow Control Meeting*, Ostritz, Germany, September 8-11.

Transition Control with Dielectric Barrier Discharge Plasmas

Dipl.-Ing. A. Duchmann
Dr.-Ing. S. Grundmann
Prof. Dr.-Ing. C. Tropea



TECHNISCHE
UNIVERSITÄT
DARMSTADT



CSI

End of Phase Report
Period 2

Award No. FA8655-08-1-3032

Abstract

The long-term objective of the project is to control natural boundary-layer transition through the use of plasma actuators. Transition delay or even suppression has its merits not only in lower wall shear stress and frictional drag of laminar as opposed to turbulent boundary layers, but transition control can be instrumental in influencing flow separation, which opens avenues for significantly influencing pressure drag and wake acoustics of bluff bodies or profiles.

The focus of the project is on understanding fundamentals of the transition control and on optimization of actuator design and operating parameters. The project is of experimental nature and is composed of three periods. During the first period, improved plasma actuators are developed for boundary-layer control. A small wind tunnel, optimized for high resolution laser optical measurements in boundary layers, was constructed and will yield precise knowledge of the flow field and volume force distribution of different actuator geometries for developing advanced actuators for transition control. These actuators will be used in a larger tunnel under pressure-gradients encountered in flight situations during the second period to enhance the design and to achieve a reliable delay of transition. The development of a feedback control circuit for active wave cancelation using pulsed plasma actuators will also be conducted in the second period. Finally, all developed technologies will be applied in the third period for in-flight experiments, demonstrating the delay of transition on the wing of a full size motorized glider.

This report complements the reports issued during period 1 and the interim report of period 2. It provides an overview over the accomplishments during the second period of the project.



Contents

1	Introduction	3
2	Flight Experiment Preparation	4
3	Improved DBD actuators	6
3.1	Influence on Boundary-Layer Stability	9
4	Active Wave Cancellation	11
4.1	Improved Flat Plate	11
4.2	Phase-Locked Techniques	11
4.3	MiniPuls 2.1	13
5	Streamwise Streak Damping	14
6	Conclusions and Outlook	17

1 Introduction

The first period of the project focussed on a better understanding of the DBD plasma actuators' working principle in quiescent air and laminar boundary layers. Recent investigations during the second year of the 3-year-project concentrated on the effect of enhanced DBD actuator configurations on laminar boundary-layer flow. The so called 'Sliding Discharge'-technology was intensively studied and the stabilizing effect of the plasma force field analyzed in comparison to standard DBD setups.

The final objective of the project is to bring DBD actuators to free-flight application. In order to conduct boundary-layer control on the Grob G109 aircraft available at Technische Universität Darmstadt, a special wing glove has to be designed, built, tested and instrumented. During period 2, a first wing glove was built and the pressure distribution measured in wind tunnel experiments. The results relate well to the design and theoretically predicted distribution.

A final goal of the project being the application of DBD actuators in free-flight, the high free-stream velocities encountered under such conditions pose a difficult environment for DBD flow control. The higher the bulk flow velocity, the lower is the ratio of the actuators momentum input compared to energy contained in the surrounding fluid, thus lowering the absolute influence. Accurate positioning of DBD actuators can help to optimize the desired effect of boundary-layer stabilization or cancelation of natural disturbances, nevertheless the magnitude of the body-force introduced by the actuator operation has to be enhanced to cope with free-flight speed environments. For this reason, the so called Sliding Discharge technique was investigated during period 2.

Additionally, the equipment and techniques for the active cancellation of Tollmien-Schlichting waves by means of DBD have been refined. A phase-locked averaging approach for the hot-wire and PIV data acquisition has been developed in period 2. These improvements enable a artificial excitation as well as the detection of small amplitude flow instabilities which are very similar to natural existing disturbances.

Besides Tollmien-Schlichting induced transition, bypass transition poses a challenging issue in terms of turbulence suppression. Steady streamwise streaks have been generated by roughness elements on a flat plate and the damping of these by DBD actuators was tested. Once again, it became obvious that for such transition control tasks, highly customized DBD actuators are necessary to obtain desirable results. The investigations during period 2 have fostered a further understanding of the DBD actuation and enable purpose-built actuators for flow and transition control.

2 Flight Experiment Preparation

The G109 motorized glider plane owned and operated by the Institute of Fluid Mechanics and Aerodynamics at Technische Universität Darmstadt is an ideal platform for transition experiments under realistic flight conditions. The project plan stipulates in-flight experiments on DBD based transition control during the upcoming third year of the project. Since such experiments need long-term preparations and acquisition of specialized hardware, work on the experimental apparatus has already been initiated during period 1. In order to transfer the DBD experiments to the in-flight environment, a special wing glove is being built. This device covers part of the original glider wing and provides space and surface for implementation of experimental equipment.



Figure 2.1: Wing glove on wing section in wind tunnel.

During the second period, a first wing glove made of epoxy-resin reinforced glass- and carbon-fibres was built and tested in a $2 \times 3\text{m}$ wind tunnel. The wing glove is mounted on a section of an original G109 wing which is vertically attached to the wind tunnel force balance. The angle of attack can be arbitrarily traversed and the wind tunnel velocity raised up to 60m/s such that flight reference conditions can be reproduced in the lab. Since it is difficult to calibrate the measurement equipment in flight, the possibility to use the fully equipped in-flight setup in the wind tunnel is an advantage of the testing capabilities at Technische Universität Darmstadt. The wing glove placed in the test section can be seen in Figure 2.1.

Figure 2.2 shows the pressure distribution measured during these wind tunnel tests for two angles of attack α on the pressure side (blue triangles) and the suction side (red circles). The measured data is compared to an analytic computation of the pressure distribution obtained from a panel method (software XFOIL). The agreement between experiment and theory is good

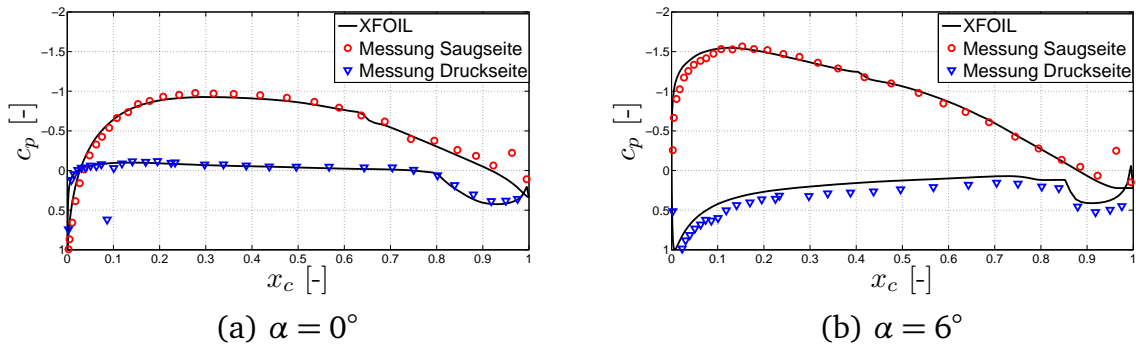


Figure 2.2: Pressure distribution of the wing glove at angles of attack of (a) $\alpha = 0^\circ$ and (b) $\alpha = 6^\circ$.

for suction and pressure sides even accounting for the transition position on the pressure side between 80% and 90% chord length. The pressure gradient along the pressure side for $\alpha = 0^\circ$ is almost zero between $x/c = 0.05$ and 0.8. For the case of $\alpha = 6^\circ$ it shows a moderate linear increase. This linear, moderate, and angle-of-attack dependent pressure gradient is ideal for the investigation of transition processes under varying conditions. The transition delay experiments with DBD actuators will first be conducted in this environment with an option to investigate the effect on the suction side later on.

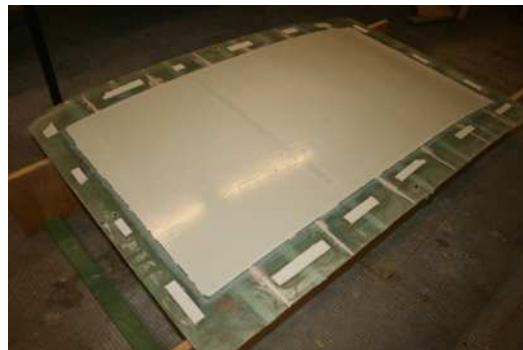


Figure 2.3: Wing glove exchangeable insert in mold.

The wing glove is composed of a fibre-composite structural frame containing 64 pressure taps distributed along the chord and an exchangeable insert section which can be instrumented according to the specific experimental needs. For the upcoming investigations on DBD actuators in flight conditions, the inserts are manufactured with cavities for the DBD electrodes and the dielectric material. Downstream of the DBD actuator position, a sensor array will enable measurement of boundary-layer instabilities and growth rates. One prototype of such an exchangeable insert providing space for a 400mm long DBD actuator is presented in Figure 2.3.

3 Improved DBD actuators

Standard DBD actuators as used in earlier experiments at the Technische Universität Darmstadt [7] and elsewhere are limited in the extent of the force field and induced flow velocities. Wilke [13] deduced a physical limit of induced wall-jet velocities for DBD actuators of around 8m/s. The momentum flux into the surrounding fluid cannot be arbitrarily raised using 'classical' DBD actuators powered by high AC voltages. On the one hand, the thickness and material of the dielectric barrier restrict the applied voltages due to electric breakdown phenomena, on the other hand, the ion acceleration is governed by the strength and extent of the electric field. Thus, new and innovative configurations are necessary to enable flow control at higher Reynolds-numbers and under free-flight conditions at velocities between 30 and 50m/s. Such configurations recently investigated cover multiple actuator arrays, nano-pulse ionization devices, advanced materials [10] or additional electrodes with DC voltage biases [9],[1]. One of the latter types, often referred to as 'Sliding Discharge (SD) Actuators', is investigated in period 2 of the project. In addition to normal two-electrode DBD actuators, such configurations include a third electrode with a high DC voltage.

The experimental setup used consists of a flat plate in the wind tunnel constructed throughout period 1. Detailed information about the flat plate as well as the test section is given in the end-of-phase report of period 1. Figure 3.1 illustrates the PIV setup which is used to measure the velocity field near the DBD actuator.

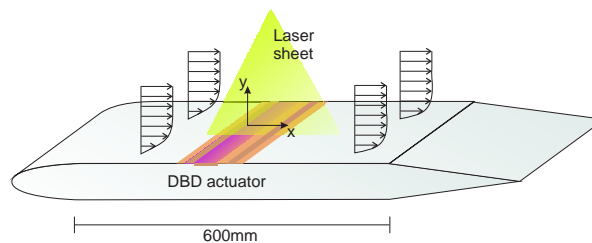


Figure 3.1: Wind tunnel and PIV setup.

The flat plate is designed to flush-mount a DBD plasma actuator at a position 250mm downstream of the flat-plate leading edge. The actuator setup is visualized in Figure 3.2. The DBD actuator used for these experiments consists of two copper tape electrodes separated by 0.3mm Kapton. The buried electrode measures 10mm width and spans the whole lateral dimension z of the test section. The exposed electrode width w is varied. The experimental coordinate system originates at the downstream edge of the exposed electrode at the wall.

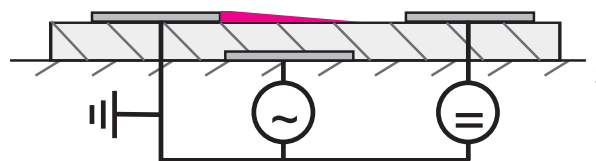


Figure 3.2: Three-electrode Sliding Discharge actuator.

In a former investigation, the effect of a single DBD actuator on low-speed boundary-layer flow was investigated [3]. These experiments revealed insights into the momentum coupling of the actuator to the boundary-layer flow, showing that the actuator power has to be adjusted to the free-stream velocity and the boundary-layer conditions. Several parameters including operation frequency, AC voltage and pulsing were investigated. For freestream velocities exceeding 9m/s, the effect on the velocity profiles obtainable from DBD actuation was hardly measurable. Therefore, this new investigation concentrates on enhancing the actuation by means of an additional electrode with DC bias. Similar setups have formerly been investigated regarding the obtainable wall-jet velocities. A detailed investigation into the effect of positive and negative potentials on the discharge behavior and created wall jets is given by Moreau et al. [9]. It is shown that the electrical properties of the Dielectric Barrier Discharge are not altered due to the addition of the constant potential at the third electrode. The power consumption can be regarded as equal to the case of the standard two-electrode setup. Dependent on the polarity of the applied DC voltage, different plasma characteristics are obtained. For positive potentials, an extended plasma region is obtained yielding higher fluid velocities. Moreau calls this setup 'Extended DBD' in order to differentiate it from applied negative potentials which show different behavior and are named 'Sliding Discharge'. For this reason it should be mentioned that in the investigations presented hereafter, only positive DC potentials are examined, nevertheless calling them Sliding Discharge (SD) actuators.

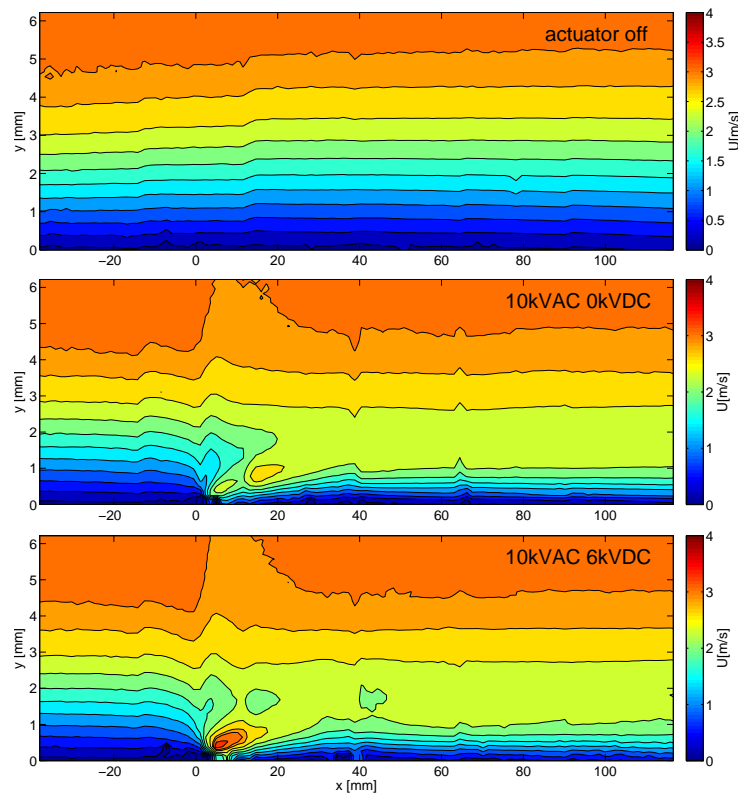


Figure 3.3: Streamwise velocity component of 3m/s flat-plate boundary-layer flow with and without DBD and SD actuation.

The AC part of the SD actuator is powered at a frequency of $f = 10\text{kHz}$ and a peak-to-peak voltage of $V_{pp} = 7.2\text{kV}$. The DC voltage V_{DC} is varied between 0kV and 12kV. To investigate

the impact of the DBD and SD actuator on boundary-layer flow, the wind tunnel is operated at various free-stream velocities between 3 and 12m/s. In Figure 3.3 the streamwise velocity component of the laminar boundary-layer flow at a wind tunnel velocity of 3m/s is shown. Results are shown for the plasma actuator being powered in the two-electrode DBD and the 3-electrode SD mode. For the case without actuation (upper figure), the isolines of the velocity run almost parallel to the wall with a slight inclination accounting for the increasing boundary-layer thickness. Turning the AC power supply on, the flow is locally accelerated whereas the overall boundary-layer thickness remains almost constant (as seen in the middle figure). The changed electric field due to the additional DC component (lower figure) leads to higher absolute velocities of the fluid between the two exposed electrodes. The exact interaction of the DC electric field with the AC component is not measurable, but the net effect of stronger momentum addition to the flow remains obvious.

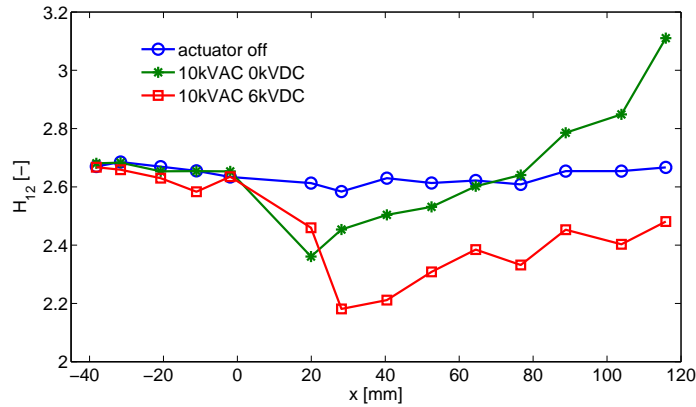


Figure 3.4: H_{12} shape factor influenced by plasma actuator ($x=0\text{mm}$).

The actuator operation decreases the momentum-loss thickness and alters the shape factor H_{12} of the boundary-layer as shown in Figure 3.4. The shape factor $H_{12} = \frac{\delta_1}{\delta_2}$ is plotted over the length of the flat plate. For the baseflow case without DBD actuation, the shape factor approaches the value of the Blasius similarity solution of $H_{12} = 2.59$. This indicates that the pressure gradient within the test section in streamwise direction $\frac{\partial p}{\partial x}$ is close to zero. If the DBD actuator is activated and the AC power supply turned on, the shape factor decreases next to the edge of the two electrodes ($x = 0$). This is consistent with investigations conducted by Grundmann [7] on the effect of DBD actuation on boundary-layer transition. The displacement thickness δ_1 as well as the momentum-loss thickness δ_2 are locally reduced due to the acceleration of the lower boundary-layer region. The decrease in shape factor indicates that the displacement thickness is reduced more pronounced than the momentum-loss thickness. Downstream of the actuator the shape factor rises again and converges towards the typical laminar-flow solution. This suggests that the effect of the actuator does not provoke transition towards turbulence but rather adds momentum to the boundary-layer, making the flow more resistant against Tollmien-Schlichting (TS) instabilities. Yet it remains unclear why the value of H_{12} for the DBD actuated case exceeds the value of the baseflow beyond $x = 75\text{mm}$. This issue has to be addressed in further experimental investigations being planned for the upcoming weeks.

3.1 Influence on Boundary-Layer Stability

The shape factor of a velocity profile is an indicator for the stability of the flow. A relation between the shape factor and the critical Reynolds number, beyond which internal instabilities in the boundary-layer are excited and eventually lead to transition, is reviewed by Grundmann [6] and illustrated in Figure 3.5. As the shape factor value is decreased, the critical Reynolds number is increased. This means that for lower shape factors the transition process which leads to turbulence will start at higher local Reynolds numbers, e.g. further downstream positions or higher flow velocities.

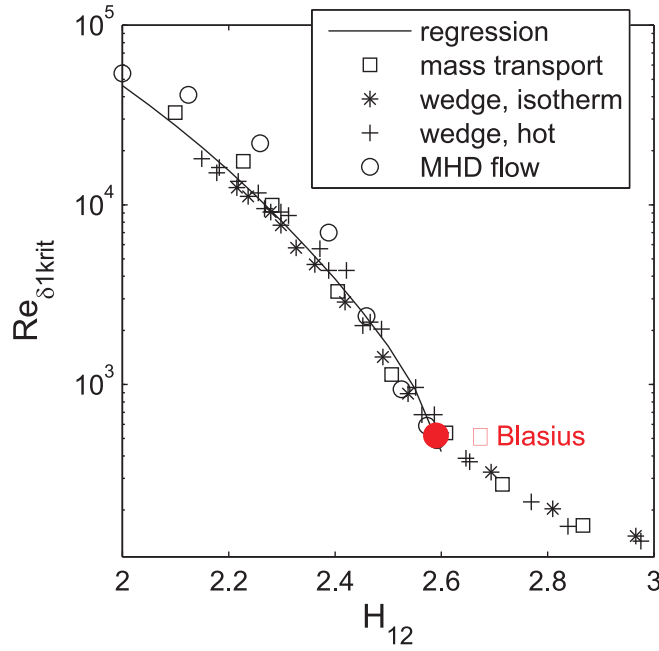


Figure 3.5: Relation between H_{12} and Re_{crit} derived from different experiments (from [6]).

Besides the H_{12}/Re_{crit} relation or analytical tools for the determination of stability properties (see [2]), a more direct way is proposed here. The stability of a laminar boundary-layer profile is highly dependent on the curvature of the streamwise velocity component, represented by the second derivative with respect to the wall-normal component $\frac{\partial^2 u}{\partial y^2}$. Negative curvature indicates a stabilized flow, which can be achieved by favorable pressure gradients, wall suction or the application of force fields. Equation 3.1 is derived from the simplified boundary-layer equations and highlights these 'stability modifiers' [5].

$$\rho v_w \left. \frac{\partial u}{\partial y} \right|_{y=0} + \left. \frac{\partial p}{\partial x} \right|_{y=0} - \left. \frac{\partial \mu}{\partial y} \frac{\partial u}{\partial y} \right|_{y=0} - \rho F = \eta \left. \frac{\partial^2 u}{\partial y^2} \right|_{y=0} \quad (3.1)$$

The velocity-profile curvature of experiments conducted at 6m/s is investigated and shown in Figure 3.6. A slightly unstable laminar boundary layer exhibits a weak positive curvature

next to the wall in the upper plot, representing the baseflow without plasma actuation. The force field created by the actuation (2-electrode DBD in the middle figure, 3-electrode SD in the lower figure) lowers the profile curvature towards negative values. In direct vicinity of the

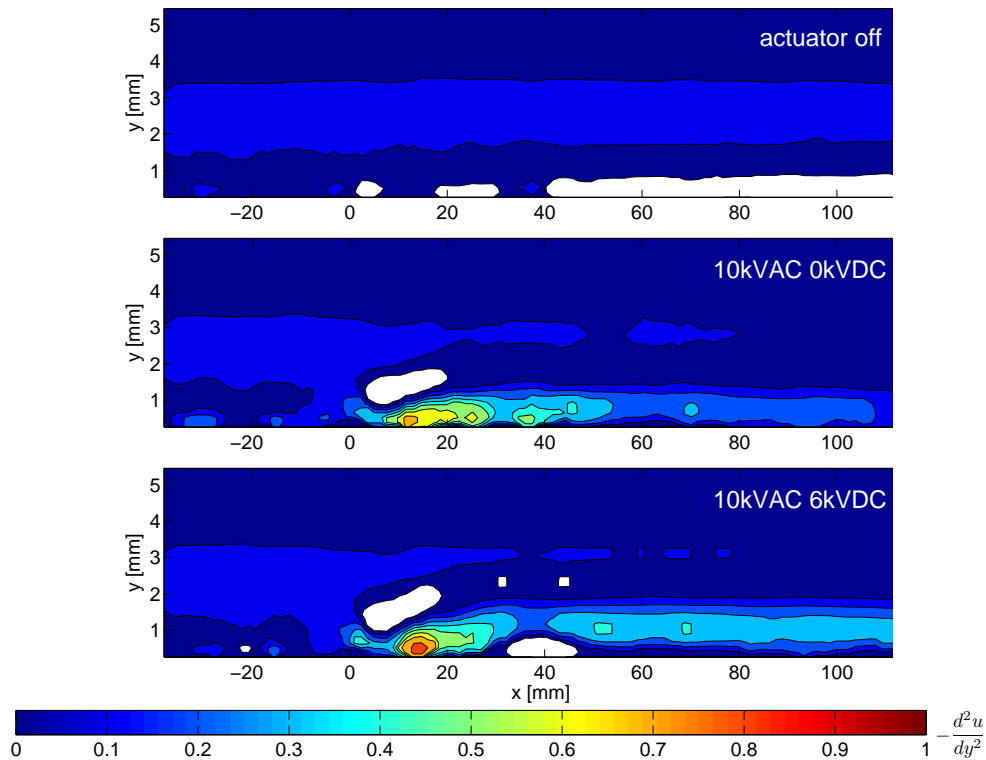


Figure 3.6: Second velocity derivative for cases with and without DBD / SD actuation.

actuator, the profiles are highly distorted, showing intrinsic instable characteristics. As the zone of abrupt forcing is left behind, the flow turns back to a more stable state indicated by the lower curvature values. This stable state is conserved along the downstream direction of the laminar boundary-layer flow. Nevertheless, the actuator force has to be adjusted correctly to the freestream velocity and stability conditions of the incoming flow, otherwise actuation can have unfavorable side effects like points of inflection in the velocity profile. An overshoot in the velocity profile, where the flow acceleration due to actuator operation exceeds the freestream velocity value, has to be avoided because it would provoke an additional point of inflection. Such a profile would be instable under most conditions and exhibits reduced critical Reynolds numbers. This observation confirms the necessity to use customized DBD actuators for transition control purposes.

4 Active Wave Cancellation

The active cancellation of Tollmien-Schlichting waves has been under investigation since period 1 of the project. Since then, considerable improvements have been achieved in the cancellation of excited boundary-layer instabilities in the wind tunnel. The final report on period 1 concluded with increased freestream velocities up to 25m/s and elaborate control algorithms for the detecting and automated cancelation of flow instabilities. In the meantime, the experimental setup could be improved in various ways.

4.1 Improved Flat Plate

In order to achieve a delayed transition by cancelation at higher speeds typical of flight environments (30-50m/s), the whole experimental setup in the wind tunnel has to be refined. A perfectly smooth flat plate made of plexiglas enables implementation of flush-mounted DBD actuators closer to the leading edge where the transition process takes place at higher speeds. An aluminium plate supports the plexiglas cover to avoid waviness in downstream direction (which would result in undetermined pressure gradient conditions) and to provide higher stiffness of the setup. Additionally, a new disturbance device for the excitation of artificial TS-waves of very low amplitudes has been implemented into the rig. The earlier experiments on wave cancelation have dealt with amplitudes far above 1% of the freestream velocity. To better resemble natural Tollmien-Schlichting waves, the new disturbance source is powered by 5 small loudspeakers which can be implemented into the in-flight setup into the future.

4.2 Phase-Locked Techniques

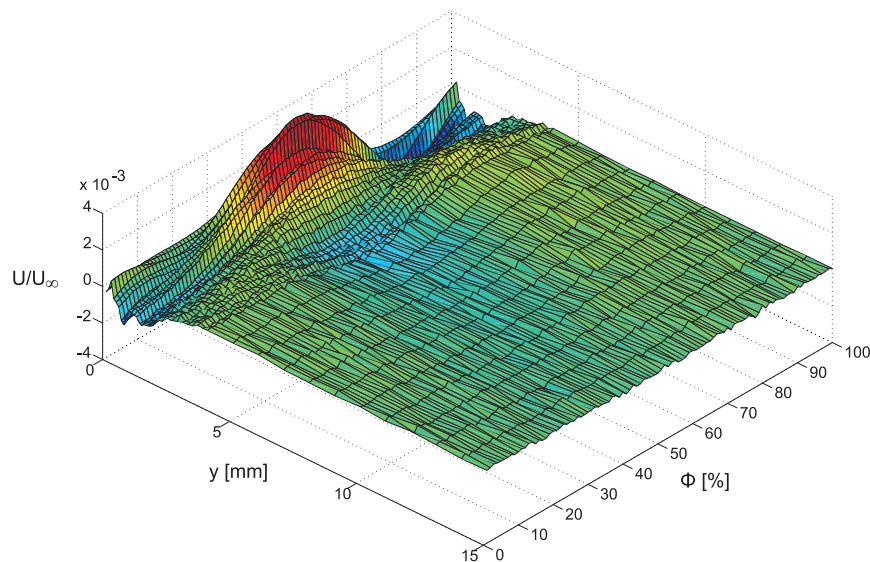


Figure 4.1: Tollmien-Schlichting wave captured by phased-locked averaging of a hot-wire signal.

For a reliable detection of the small amplitude disturbances, the signal-to-noise ratio of standard hot-film sensors is hardly sufficient. Even the use of hot-wire probes, traverseable along

the wall-normal direction to gather boundary-layer profiles, makes it difficult to differentiate between the TS-wave flow fluctuations and free-stream turbulence due to the wind tunnel operation. Keeping in mind the usual freestream turbulence levels encountered in windtunnel experiments around 0.5%, the disturbance amplitudes which are to be measured are of the same order of magnitude as the turbulent noise, especially in the boundary-layer close to the walls. In order to correlate the excited TS-disturbances to the measurements, a phase-locked analysis of the hot-wire signal is necessary. The hot-wire data as well as the disturbance source input signal are measured simultaneously, enabling phase-locked averaging of the hot-wire signal during the post-processing. This approach yields a better resolution of the wave structures by omittance of noise. An exemplary result of one TS-wave captured approximately 100mm downstream of the disturbance source is presented in Figure 4.1. The colors as well as the vertical axis represent the wave amplitude, non-dimensionalized with the freestream velocity. The lateral axes are the wall-normal coordinate y and the phase Φ (in % of one wave period). The wave shown here exhibits an amplitude of 0.4% of the freestream velocity. Although the wave has a very small amplitude, the fluctuation maximum close to the wall as well as the phase shift of the velocity fluctuation at higher y is resolved with this technique.

Another approach is to use a phase-locked technique on the aquisition of PIV data (compare Chapter 3). A graduate student project is currently running to enable phase-averaged flow measurements next to the DBD actuator. The scope of the project is to identify the effect of the DBD on an incoming, artificially excited Tollmien-Schlichting wave. First results cover the excited TS-waves without DBD operation. The velocity fluctuation field and the convective transport of the disturbance structure is illustrated in the raw results of Figure 4.2. The colors

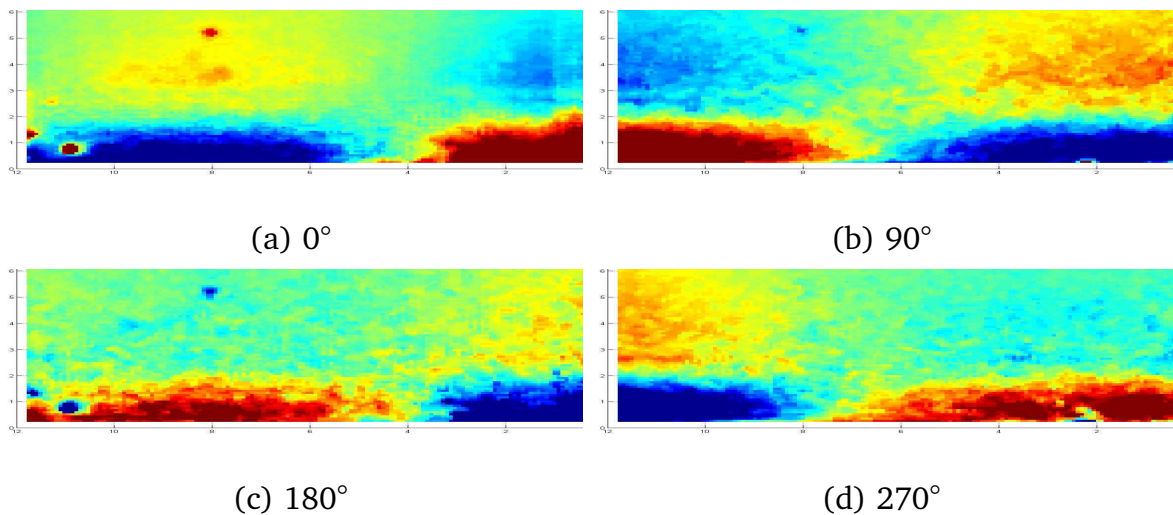


Figure 4.2: TS-waves captured by PIV imaging at different phase relations.

illustrate the velocity fluctuation, red indicating 1% of the freestream velocity and blue -1% of that value. The displacement of the wave amplitude cores translates to the convection of the instability at about $1/3$ of the wind tunnel speed. Again, the phase-shift of the velocity fluctuations at the edge of the boundary-layer that is characteristic for TS instabilities is well observable.

With this technique, an analysis of the spatial development of TS-waves under influence of DBD actuation will be achievable. This is the enabling technology to observe the time-resolved

effect of pulsed and continuously operated DBD actuators on TS-waves. It is important to note that these results illustrate a wave amplitude of 1%, such that the technique can be applied to the characterization of natural Tollmien-Schlichting waves.

4.3 MiniPuls 2.1

Numerical investigations by Quadros [11] have shown that TS-waves can optimally be canceled by anti-phase sinusoidal modulation of the DBD force. Up to now, the power source for the DBD could only be switched on and off at the frequency of the incoming wave. The newly developed MiniPuls 2.1 by *GBS Elektronik*, which is illustrated in Figure 4.3, enables a sinusoidal modulation of the high-voltage for the Dielectric Barrier Discharge. The advantage of this is



Figure 4.3: MiniPuls 2.1 device.

illustrated in Figure 4.4. Whereas the old equipment only allowed a rectangular modulation of the force in the time frame of the TS-wave period T_{TS} (a), the new equipment is capable of producing a perfect counter-phase sinus force (b). The single pulses at the high driving frequency of f_{pl} resemble the driving mechanism of the DBD which leads to a quasi-steady integral force production. If this signal is modulated correctly, flow disturbances can effectively be canceled.

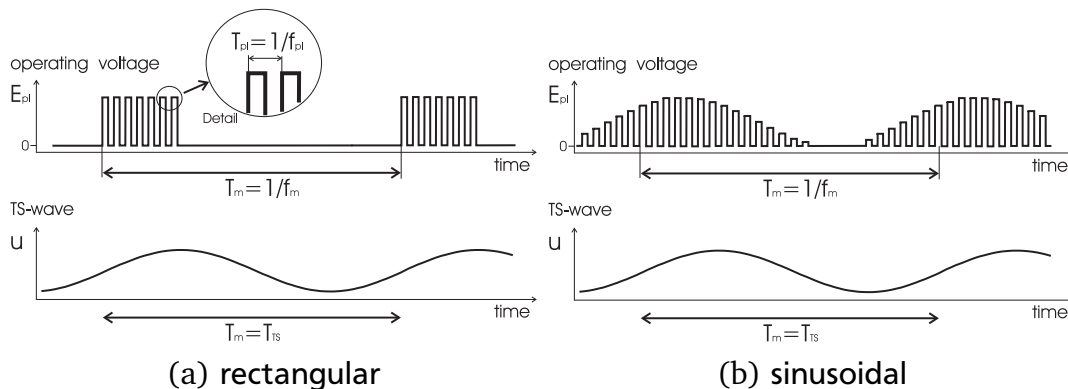


Figure 4.4: Modulation of the actuator force.

5 Streamwise Streak Damping

Since the Tollmien-Schlichting wave scenario can be influenced effectively by means of DBD actuator, the question arises if other transition mechanisms can also be suppressed. The transition mechanism that is dominant under conditions of high freestream turbulence or external vibration and acoustic contamination is the so called 'bypass transition'. The receptivity mechanism leading to transition by growth of TS waves is bypassed and external turbulence enters the boundary layer directly. Secondary instabilities are created in the form of streamwise streaks and counter-rotating vortices. Our aim was to diminish the effect of such instabilities by counteracting the vortices in the boundary-layer. Under realistic conditions, such instabilities form randomly and can exhibit transient growth and decay. In order to understand how DBD actuators can be applied to cancel these instabilities in a first attempt, an experimental setup has to be designed which enables a spatially and temporally steady state of the flow structures. For such investigations, the installation of distributed roughness elements on a flat plate has proven beneficial. White [12] and Fransson [4] have thoroughly investigated the spatial development of the structures created by a setup illustrated in Figure 5.1.

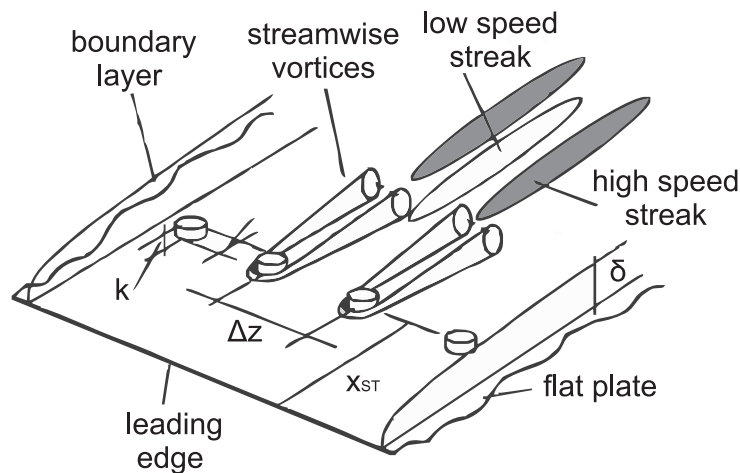


Figure 5.1: Setup using roughness elements and generated flow structures (after [4]).

The wake of the roughness elements leads to a formation of vortices which effect a momentum transfer between the boundary-layer and the freestream. In this fashion, zones of low- and high-speed fluid, called streaks, are distributed symmetrically behind the elements. The shear layers forming between the streaks lead to transition to turbulence, therefore a damping of the velocity differences is desirable. Inspired by the work of Hanson and Lavoie [8], DBD actuators are used to apply a force in spanwise direction, thereby counteracting the vortices and damping the streak structures. The DBD force acting on the flow not only depends on the input power but also on the length of the DBD in streamwise direction. Therefore, a multi-dimensional optimization problem has to be solved to enable adequate damping of the disturbances. In addition to that, it has become clear during the measurements that the position of the actuators relative to the flow structures is also of importance. Therefore, different actuator geometries, positions and power levels have been investigated. In Figure 5.2 the physical dimensions of the setup as well as two different actuator geometries are presented.

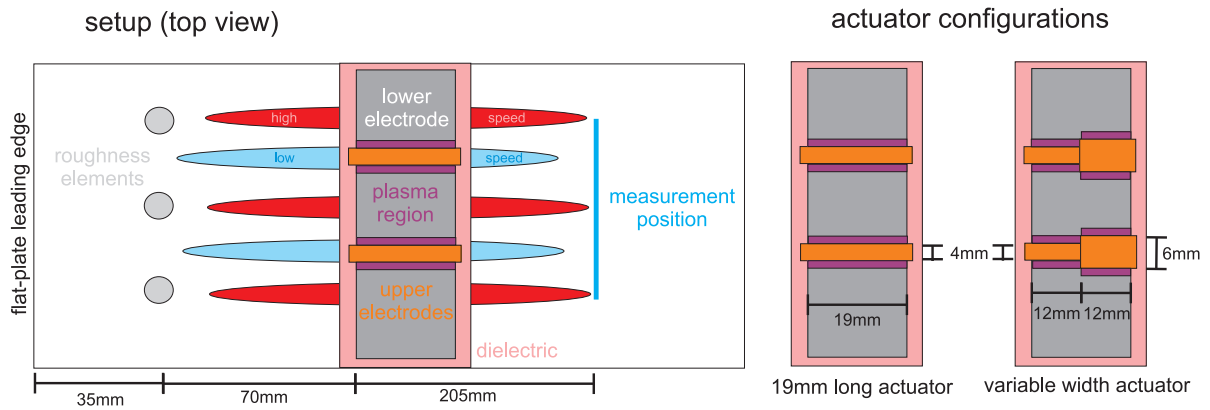


Figure 5.2: Setup with different actuator geometries.

Figure 5.3 shows some results from the hot-wire measurements in the spanwise/wall-normal plane downstream of the roughness elements. The baseflow case (a) without DBD actuation clearly shows the high- and low-speed streaks visible in the red and blue areas. The streak amplitudes are in the range of 5% of the freestream velocity (10m/s in this case), indicated by the colorbar.

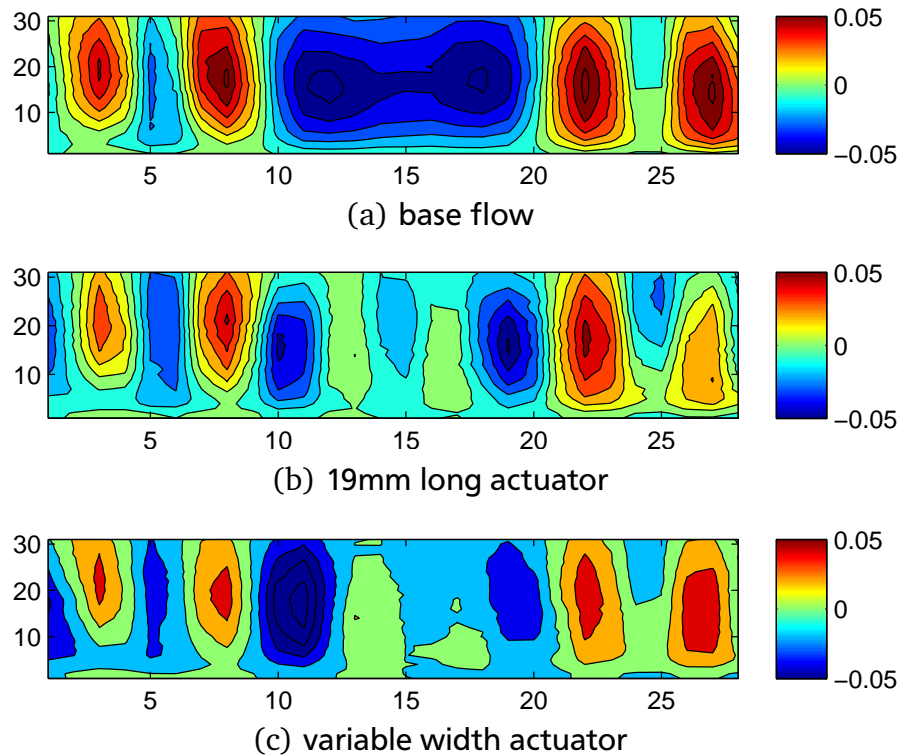


Figure 5.3: Streak velocity amplitudes for different DBD operation parameters.

An adequately positioned, 19mm long DBD actuator is applied and the output power adjusted to the flow conditions (9,9kHz, 3.5kV) for the results in (b). The streak amplitudes are dampened slightly, the primary structures are reduced and the extent decreased. Especially the low-speed streak in the middle of the figure is broken up and amplitudes reduced to about 1%. In order to further enhance the damping of the streak magnitudes, a DBD actuator with 2 upper electrodes of different width (4 and 6mm) is applied (c). The setup of this actuator can

be reviewed in Figure 5.2. If this actuator is powered at 3.8kV, the flow structures are further diminished and the flow is more homogenous. The inhomogeneity of the velocity distribution can be expressed by the integral of the velocity fluctuations over the investigated domain, $A = \int u' dy dz$. The values for this integral approach resembling the standard deviation of the velocities from the mean flow are listed in Table 5.1.

Configuration	A	%
(a)	2.61	100
(b)	1.97	75
(c)	1.61	62

Table 5.1: Variation of the inhomogeneity of the flow field.

The results show that DBD actuators can be used to dampen streamwise streaks in laminar boundary-layer flows. The investigations on this topic are still in progress and will provide insight to which extent DBD can be used to cancel such instabilities. The relatively simple setup of roughness elements on a surface may prove applicable for the in-flight experiments on a dedicated wing glove.

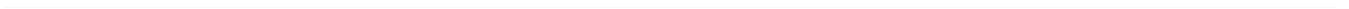
6 Conclusions and Outlook

Various experimental setups have been built and investigated to improve the knowledge about how DBD actuators can be used for transition control. This led to the following conclusions:

- The equipment for the in-flight experiments will soon be available, an identical wing-glove as will be used for the DBD investigations has been tested in the wind tunnel and the pressure profile determined. The exchangeable inserts are being instrumented with DBD actuators and sensor equipment and a first wind tunnel experiment with DBD on the wing glove should be available by the end of 2010.
- Sliding Discharge actuators can effectively stabilize a laminar boundary-layer and show enhanced transition control authority over standard DBD actuators. The additional DC potential increases the extent and magnitude of the force field.
- The experimental equipment for the mid-size wind tunnel investigations has been improved by the construction of a new flat plate, a more sophisticated disturbance source for excitation of instabilities and new DBD power supply equipment. The new MiniPuls enables sinusoidal force modulation for better active cancelation of TS waves and a phase-locked sensing approach increases the signal-to-noise ratio for better analysis of the cancelation result.
- Streamwise streaks were created in the small wind tunnel to identify possibilities of damping these instabilities by DBD actuation. A streak amplitude reduction, homogenizing the flow by 38%, has been obtained in a first parametrical study. With more detailed adjustment of the specially designed DBD actuators, further enhancements are expected.

During the next months, the DBD wing glove will be finished and tested in the 2x3m wind tunnel. Active wave cancelation will be conducted on the flat-plate experiment in the mid-size wind tunnel and the investigation of boundary-layer stabilization by steadily operated DBD and Sliding Discharge actuators will be continued in the small-scale wind tunnel. Until the end of project period 3, DBD actuators will be applied on the wing glove in flight experiments. The obtainable effect on transition under realistic flight conditions will be evaluated and presented in the next report.

The new phase-locked measurement techniques enable exact determination of the effect of steadily operated and pulsed DBD actuators on boundary-layer instabilities. The optimization of DBD actuators for transition control can only be successful if these mechanisms are thoroughly understood. The current improvements of the measurement techniques enable the design of purpose-built, customized DBD actuators for the in-flight investigations.



Bibliography

- [1] Borghi, C. A., Carraro, M. R., Cristofolini, A. & Neretti, G. (2008) Electrodynamic interaction induced by a dielectric barrier discharge *Journal of Applied Physics*, **103**, 063304.
- [2] Duchmann, A., Reeh, A., Kriegseis, J., Tropea, C. (2009): Linear Stability Analysis for Manipulated Boundary-Layer Flows using Plasma. *Seventh IUTAM Symposium on Laminar-Turbulent Transition*, Stockholm, Sweden, June 23-26.
- [3] Duchmann, A., Kriegseis, J., Grundmann, S., Tropea, C. (2009): Customizing DBD Actuators for Flow-Control Applications using PIV. *8th International Symposium on Particle Image Velocimetry*, Melbourne, Australia, August 25-28.
- [4] Fransson, J., Brandt, L., Talamelli, A. & Cossu, C. (2004): Experimental and theoretical investigation of the nonmodal growth of steady streaks in a flat plate boundary layer. *Physics of Fluids*, Vol. 16, No. 10.
- [5] Gad-El-Hak, M. (2000) Flow Control *Cambridge University Press*, ISBN 0-521-77006-8.
- [6] Grundmann, S. (2008): Transition Control using Dielectric-Barrier Discharge Actuators. *Ph.D. Thesis* Institute of Fluid Mechanics and Aerodynamics, TU Darmstadt.
- [7] Grundmann, S., Tropea, C. (2009): Experimental Damping of Boundary-Layer Oscillations using Plasma Actuators. *International Journal of Heat and Fluid Flow*, **30**, Issue 3, 394-402.
- [8] Hanson, R.E., Lavoie, P., Naguib, A.N. & Morrison, J.F. (2009): Control of transient growth induced boundary layer transition using plasma actuators. *Seventh IUTAM Symposium on Laminar-Turbulent Transition*, Stockholm, Sweden, June 23-26.
- [9] Moreau, E., Sosa, R. & Artana, G. (2008): Electric wind produced by surface plasma actuators: a new dielectric barrier discharge based on a three-electrode geometry. *Journal of Physics D: Applied Physics*, 41.
- [10] Opaitis, D. F., Zaidi, S. H., Schneider, M. N. & Miles, R. B. (2009) Improving Thrust by Suppressing Charge Build-Up in Pulsed DBD Plasma Actuators. *47th AIAA Aerospace Science Meeting*, Orlando, Florida, January 5-8, AIAA 2009-487.
- [11] Quadros, R., Grundmann, S., Tropea, C. (2008): Numerical Simulations of the Transition Delay Using Plasma Actuators. *7th International ERCOFTAC Symposium on Engineering Turbulence Modelling and Measurements ETMM7*, Limassol, Cyprus, June 4-6.
- [12] White, E.B. & Ergin, F.G. (2003): Receptivity and Transient Growth of Roughness-Induced Disturbances. *33rd AIAA Fluids Dynamics Conference*, Orlando, Florida, June 23-26.
- [13] Wilke, B., Hoffer, P.A., Rosemann, H. (2009): Experiment-based fluidic modeling of plasma actuators. *Experiments in Fluids* (to be published).